



# Solidification using smoothed particle hydrodynamics

Joseph J. Monaghan <sup>a,\*</sup>, Herbert E. Huppert <sup>b</sup>, M. Grae Worster <sup>b</sup>

<sup>a</sup> *School of Mathematical Sciences, Monash University, Australia*

<sup>b</sup> *Institute for Theoretical Geophysics, Centre for Mathematical Sciences, Wilberforce Rd., Cambridge CB3 0WA, UK*

Received 29 March 2004; received in revised form 24 September 2004; accepted 11 November 2004

Available online 25 February 2005

---

## Abstract

We show how the numerical particle method smoothed particle hydrodynamics (SPH) can be used to simulate the freezing of one and two-component (binary alloy) systems. We first study the freezing of a pure liquid, and compare our computations against exact results for one and two dimensional systems, including cases where there are point sources and the boundary of the system is irregular. The agreement with theory, where it is available, is very satisfactory. We then consider a two-component system which is initially entirely liquid and model it by a set of liquid SPH particles together with a set of virtual solid SPH particles which initially have no mass. During the thermal evolution and solidification of the system, mass is transferred from the liquid SPH particles to the ice (solid) SPH particles. For a binary melt, as the volume fraction of the solid increases the composition of the liquid is enriched in the component of the alloy that does not form the solid phase. In the case of salty water, this component is the salt. We find that the variation of temperature and liquid composition calculated with SPH is in close agreement with previous theories of mushy layers and gives similar agreement with experiment. In this initial study we simplify the calculations by assuming the solid particles remain in the position where they are formed: a good approximation for the case where the solution is cooled from above to form ice leaving behind a relatively light residual liquid, or cooled from below leaving behind a relatively heavy liquid. We compare our results with experiments on the freezing from below of an aqueous sodium nitrate solution [Nature 314 (1985) 703], and find that the agreement is very satisfactory.

© 2005 Published by Elsevier Inc.

---

## 1. Introduction

Solidification from multi-component solutions is an important process in geology and industry. In the former it plays a major part in the formation of mineral deposits, and in the latter it is a fundamental

---

\* Corresponding author. Tel.: +61 3 9905 4431; fax: +61 3 9905 3867.

E-mail address: [joe.monaghan@sci.monash.edu.au](mailto:joe.monaghan@sci.monash.edu.au) (J.J. Monaghan).

process in problems as diverse as the refining of metals from ores and the preparation of single crystals of silica for the semi-conductor industry.

The simplest of the solidification problems is the Stefan problem where the material is pure. A commonplace example is the formation of ice by the cooling of pure water. If the material is stationary and homogeneous with material properties independent of temperature, and the boundaries are sufficiently simple, the calculation of the interface between phases can be reduced to the evaluation of an algebraic eigenvalue relationship [6]. However, if the material properties depend on temperature, or the boundary of the domain is complex, numerical methods must be used.

Early numerical simulations were concerned with simple homogeneous fluids of constant composition. In order to capture a moving interface on a fixed numerical grid, Oleinik [17] replaced the temperature by the enthalpy as the dependent variable and introduced a smoothing function to mimic the discontinuity in enthalpy (due to latent heat) across the interface. This idea formed the basis of the finite difference calculation of the effect of distributed heat sources on melting [2] and the calculation by Crowley and Ockendon [5] of melting in the presence of time-dependent heating. These calculations assumed that the temperature only varied in one dimension.

If the material is not homogeneous, as in the case of solidifying salty water, the heat conduction problem must be enlarged to include composition changes between the phases. Numerical calculations of the two-dimensional solidification of binary alloys were made by Ungar and Brown [26] using boundary conforming finite elements. Improvements of this method allowed more complicated problems associated with deep and deformed cells to be simulated [25,23]. However, these calculations were confined to simple cellular topologies which may be relevant to small scale laboratory experiment but are seldom directly applicable to larger scale natural situations. Furthermore, the particle equivalent of the heat conduction and concentration diffusion equations can be designed so that discontinuities in the material properties can be handled easily without explicit reference to the interface. A common feature of current methods is to smooth interfaces. Juric and Tryggvason [14] used such smoothing to replace delta functions by continuous functions in a similar manner to Peskin [19] who simulated flow within an elastic membrane. A detailed review of this technique is given by Tryggvason et al. [22].

Apart from the problem of pure solidification or melting, there are further problems associated with solidification in the presence of fluid flow [9]. A typical example is the growth of dendrites in shear flow. The two dimensional case has been simulated by Tonhardt and Amberg [21], Beckerman et al. [3] and Juric [13] using interface smoothing.

A further complication is that the change in phase can produce buoyancy forces which result in bulk motion. For an interesting and comprehensive discussion of these problems in a geological context see Huppert [10,11].

In the present paper, we explore the application of the particle method smoothed particle hydrodynamics (SPH; for a review see [16]) to solidification. We choose this technique because it is a gridless method which can be used even when the domain is very complicated. Furthermore, the particle equivalent of the heat conduction and concentration diffusion equations can be designed so that discontinuities in the material properties can be handled easily without explicit reference to the interface between phases. This interface can be found at any time by delineating the boundary between sets of particles representing different phases. Enthalpy methods also have this advantage (for a general reference see [8]) but they achieve it by writing the heat conduction equation so that it involves the rate of change with time of a discontinuous enthalpy function rather than the rate of change of the thermal energy. The problems associated with this procedure are discussed in detail by Crank [8].

A possible disadvantage of particle methods is that, during the solidification, the liquid particles may produce a small mass of solid (ice) during any time step. It would be natural to construct a new SPH ice particle for each such mass, but that would produce so many small mass particles during the evolution that the calculations would be paralyzed. In this paper, we evade this problem by extending SPH to include

a set of ice particles which initially have no mass (and are therefore called virtual), but increase in mass as the system is cooled according to the thermodynamics of the phase change. The small parcels of ice that are formed in any time step are added to these ice particles which increases their mass. The initial virtual ice particles therefore become real ice particles as the calculation proceeds. Typically, at any time there are both real and virtual ice particles, but the total number remains constant.

A natural consequence of the formation of the ice SPH particles is a region of ice and liquid SPH particles between the pure solid and pure liquid phases which mimics the region of interpenetrating solid bathed in interstitial liquid (the mush) found in all experimental situations of solidification of binary alloys. We will show that the predictions of SPH are very similar to those based on mushy layer theory [28,29].

The aim of this paper is to lay the foundation for the application of SPH to problems with phase changes and, in particular, to problems involving solidification, melting and their associated fluid flow. The full range of problems is large and we confine our present study to problems without fluid motion. We first derive the SPH equations for the Stefan problem associated with a fluid with a single composition. We then derive SPH equations for the freezing of binary solutions and apply them then to the freezing from below of a sub-eutectic aqueous solution of sodium nitrate which has been investigated experimentally by Huppert and Worster [12].

## 2. Heat conduction and salt diffusion

The fundamental field equations describing solidification are the heat conduction and composition diffusion equations. We begin by giving the SPH forms of these equations.

### 2.1. The SPH heat conduction equation

The heat conduction equation is

$$c_p \frac{dT}{dt} = \frac{1}{\rho} \nabla(\kappa \nabla T), \quad (2.1)$$

where  $T$  is the absolute temperature,  $c_p$  is the heat capacity per unit mass at constant pressure,  $\rho$  the density,  $\kappa$  the coefficient of thermal conductivity, and  $d/dt$  the derivative following the motion.

Because the heat conduction equation involves second derivatives it is necessary to choose an SPH form with care. If this is not done, the disorder that often occurs with SPH particles in a problem involving motion will result in second derivatives with large errors. In addition, any such equations should guarantee that energy and matter are conserved for isolated systems, and ensure that the conduction and diffusion lead to an increase in the entropy of the system. A suitable form can be found by starting with the integral [7]

$$\frac{1}{\rho(\mathbf{r})} \int [\kappa(\mathbf{r}') + \kappa(\mathbf{r})][T(\mathbf{r}) - T(\mathbf{r}')]F(\mathbf{r} - \mathbf{r}', h) d\mathbf{r}', \quad (2.2)$$

where  $d\mathbf{r}'$  is a volume element and  $h$  is a length scale. The function  $F$  is defined by

$$\mathbf{r}F(\mathbf{r}, h) = \nabla W(\mathbf{r}, h), \quad (2.3)$$

where  $W(\mathbf{r}, h)$  is an interpolation kernel and for the usual choices of  $W$  we find  $F \leq 0$  and  $F(-\mathbf{r}, h) = F(\mathbf{r}, h)$ . In this paper, we use the cubic spline kernel [16] which has compact support and vanishes for  $r \geq 2h$ . Values of  $h$  in the range  $\Delta p \leq h \leq 1.5\Delta p$ , where  $\Delta p$  is the particle spacing, give satisfactory results. If the integrand in (2.2) is expanded in a Taylor series around  $\mathbf{r}$ , and terms of  $O(h^2)$  are neglected, we recover the right hand side of (2.1).

The SPH method allows us to approximate volume integrals by summation over particles according to the rule

$$\int A(\mathbf{r}')d\mathbf{r}' \sim \sum_b m_b \frac{A_b}{\rho_b}, \tag{2.4}$$

where  $m_b$  is the mass assigned to particle  $b$ ,  $\rho_b$  is the density and  $A_b$  is the value of the function  $A$  at particle  $b$ .

If we apply this rule to the integral (2.2) and take  $\mathbf{r}$  to be the coordinate  $\mathbf{r}_a$  of particle  $a$ , the SPH form of (2.1) for any particle  $a$  becomes

$$c_{p,a} \frac{dT_a}{dt} = \sum_b \frac{m_b}{\rho_a \rho_b} (\kappa_a + \kappa_b) (T_a - T_b) F_{ab}, \tag{2.5}$$

where the coordinate of particle  $b$  is  $\mathbf{r}_b$  and  $F_{ab}$  denotes  $F(\mathbf{r}_{ab})$  with the notation (used throughout this paper for vectors)  $\mathbf{r}_{ab} = \mathbf{r}_a - \mathbf{r}_b$ . The summation is formally over all particles, but because the kernel  $W_{ab}$  and hence  $F_{ab}$  have compact support, only near neighbours contribute to the summation.

The previous form of the heat conduction equation (2.5) does not guarantee that the heat flux will be continuous when  $\kappa$  is discontinuous. Cleary and Monaghan [7] show from an analysis of the finite difference case that this problem can be solved by replacing  $(\kappa_a + \kappa_b)$  by

$$\frac{4\kappa_a \kappa_b}{(\kappa_a + \kappa_b)}. \tag{2.6}$$

The heat flux is then continuous even with jumps by a factor  $10^3$  in  $\kappa$  across 3 particle spacings [7]. A slightly different  $\kappa$  term based on similar ideas gives satisfactory results for jumps in  $\kappa$  by a factor  $10^9$  [18]. However, because the very simple form (2.6) gives excellent results for the normal range of material properties we use it in this paper. The final heat conduction equation we use is therefore

$$c_{p,a} \frac{dT_a}{dt} = \sum_b \frac{m_b}{\rho_a \rho_b} \frac{4\kappa_a \kappa_b}{(\kappa_a + \kappa_b)} (T_a - T_b) F_{ab}. \tag{2.7}$$

Cleary and Monaghan [7] showed that this SPH form of the heat conduction equation had similar accuracy to finite difference methods and was not sensitive to the particle disorder that occurs in some SPH calculations. In addition, heat conduction problems with discontinuous  $\kappa$ , and with  $\kappa$  varying with  $T$ , were accurately integrated.

If the particles are thermally isolated (so they can only exchange heat amongst themselves) then (2.2) shows (noting that  $F_{ab} = F_{ba}$ ), that the total heat content

$$\sum_a m_a c_{p,a} T_a \tag{2.8}$$

is constant.

### 2.2. Heat conduction with sources or sinks

When the system contains point sources or sinks (2.1) becomes

$$\rho c_p \frac{dT}{dt} = \nabla(\kappa \nabla T) + \sum_k Q_k \delta(\mathbf{r} - \mathbf{R}_k), \tag{2.9}$$

where  $Q_k$  denotes the strength of the source or sink and is negative for a sink.  $\mathbf{R}_k$  denotes the position of source/sink  $k$  and  $\delta$  denotes a Dirac delta function. The SPH equation corresponding to this becomes

$$c_{p,a} \frac{dT_a}{dt} = \sum_b \frac{m_b}{\rho_a \rho_b} \frac{4\kappa_a \kappa_b}{(\kappa_a + \kappa_b)} (T_a - T_b) F_{ab} + \frac{1}{\rho_a} \sum_k Q_k \zeta_k W(\mathbf{r}_a - \mathbf{R}_k), \quad (2.10)$$

where the delta function has been replaced by a smoothing kernel which is consistent with the smoothing of the original continuum equation and, to ensure that the rate of change of thermal energy due to the source is correct, we have introduced a normalizing factor  $\zeta_k$  for source  $k$  defined by

$$\frac{1}{\zeta_k} = \sum_b \frac{m_b}{\rho_b} W(\mathbf{r}_b - \mathbf{R}_k, h), \quad (2.11)$$

where the right hand side is an SPH estimate of the constant 1 at the position of the source. We then find that, for an adiabatic enclosure,

$$\frac{d}{dt} \left( \sum_a m_a c_{p,a} T_a \right) = \sum_k Q_k \quad (2.12)$$

as expected.

### 2.3. Salt diffusion

We denote the mass fraction of salt by  $C$  so that the mass of salt in a mass  $M$  of liquid is  $CM$ . The diffusion of the salt is given by an equation similar in form to the heat conduction equation namely

$$\frac{dC}{dt} = \frac{1}{\rho} \nabla(D\nabla C), \quad (2.13)$$

where  $D$  is the coefficient of diffusion with dimensions of  $ML^{-1}T^{-1}$ . The time scale for salt diffusion over a distance  $\ell$ , is  $\rho\ell^2/D$  which is almost a factor 100 greater than that for heat diffusion for the materials considered in this paper.

The SPH form of this equation follows in the same way as for the heat conduction equation. We find that the rate of change of the concentration  $C_a$  of particle  $a$  is given by

$$\frac{dC_a}{dt} = \sum_b \frac{m_b}{\rho_a \rho_b} \frac{4D_a D_b}{(D_a + D_b)} (C_a - C_b) F_{ab}. \quad (2.14)$$

The combination of  $D$  in the SPH equation ensures that the flux of material across an interface between two materials with different diffusion coefficients is constant. The total mass of salt  $\sum_a C_a m_a$  is conserved by the SPH equation.

#### 2.3.1. The increase of entropy

It is useful first to note that the contribution of a particular particle  $b$  to the rate of change of the temperature of particle  $a$  is given by

$$\frac{m_b}{\rho_a \rho_b} \frac{4\kappa_a \kappa_b}{(\kappa_a + \kappa_b)} (T_a - T_b) F_{ab}. \quad (2.15)$$

Recalling that  $F_{ab} \leq 0$  we find that, if  $T_a > T_b$ ,  $T_a$  decreases as it should.

The SPH conduction equation also results in entropy increasing in the absence of sources. If  $S$  is the total entropy of the system then

$$\frac{dS}{dt} = \sum_a m_a \frac{ds_a}{dt} = \sum_a \frac{m_a}{T_a} \frac{dq_a}{dt}, \quad (2.16)$$

where  $s_a$  is the entropy/mass of particle  $a$ ,  $q_a$  is the heat content/mass of particle  $a$  and  $T$  is the absolute temperature. From Eq. (2.7), with an interchange of labels, we find that

$$\frac{dS}{dt} = \frac{1}{2} \sum_a \sum_b \frac{m_a m_b}{\rho_a \rho_b} \frac{4\kappa_a \kappa_b}{(\kappa_a + \kappa_b)} \left( \frac{1}{T_a} - \frac{1}{T_b} \right) (T_a - T_b) F_{ab}. \tag{2.17}$$

Since  $F_{ab} \leq 0$  we deduce that  $dS/dt \geq 0$ .

When the composition changes there is a further contribution to the entropy. To deduce this we first divide (2.10) by  $C_a$ . If the resulting equation is summed over  $a$ , and added to the same expression with the labels interchanged, we find that

$$\frac{d}{dt} \sum_a m_a \ln C_a = \sum_a \sum_b m_a m_b \frac{4D_a D_b}{(D_a + D_b)} \left( \frac{1}{C_a} - \frac{1}{C_b} \right) \frac{(C_a - C_b)}{\rho_a \rho_b} F_{ab} \geq 0, \tag{2.18}$$

which is the increase of entropy resulting from composition changes.

### 2.3.2. Boundary and interface conditions

We assume that the heat content of the system only changes because the particles lose or gain heat through a boundary, although it would be possible to include sources of heat. For the problems considered here the boundaries are maintained at fixed temperatures or adiabatic, or periodic conditions are used.

There is no need to place a special condition on the gradient of the temperature at the boundary to satisfy these conditions if SPH is used. If all the boundaries are adiabatic then the particles interact amongst themselves and the symmetry of the SPH conduction equation ensures that the system conserves its thermal energy as shown above. If one or more boundary curves have fixed temperatures, the SPH particles on the boundaries are included in the heat conduction equation so that the heat transferred to the boundary during a time step can be calculated. After this is done the temperatures of the boundary particles are set back to the specified boundary temperatures for the next time step. The heat transferred to the boundary particle can be calculated from the temperature change. Cleary and Monaghan [7] noted that near boundaries the SPH interpolation can give errors of a few percent and they made corrections to the density near the boundary to compensate for this. In the present tests no such correction is made. The equation for the concentration of solute  $C$  is integrated assuming that no solute escapes from the domain. This, like the adiabatic condition, does not require any special boundary condition. Periodic boundaries are implemented using ghost particles.

As noted earlier, SPH calculations do not need special interface conditions. The SPH particles exchange heat and material with neighbouring particles whether they are of the same or different phase. In the technique of Juric and Tryggvason [14] the interface conditions are included as special source terms arising from the interface giving more complicated equations than with the SPH method.

### 2.3.3. Time stepping

For simplicity, the problems considered in this study were integrated using an explicit Euler time stepping scheme, which for (2.2) takes the form

$$T_a^{n+1} = T_a^n + \frac{\Delta t}{c_{pa}} \sum_b \frac{m_b}{\rho_a \rho_b} \frac{4\kappa_a \kappa_b}{(\kappa_a + \kappa_b)} (T_a^n - T_b^n) F_{ab}, \tag{2.19}$$

where  $T^n$  denotes the temperature at the  $n$ th time step. We use an analogous time stepping procedure for the equation for  $C$ . Other, more efficient, time stepping schemes could be used, but they are not necessary for the problems we consider in this paper because computational demands are light.

Cleary and Monaghan [7] found that for an improved Euler scheme the stability condition for the time step  $\Delta t$  for systems in two dimensions was

$$\Delta t = 0.15c_p\rho h^2/\kappa, \quad (2.20)$$

where  $h$  is the resolution length of the kernel. The same time-step condition is used here. Since typically  $h = 1.2\Delta p$  where  $\Delta p$  is the particle spacing, this time step limit is close to that for explicit Euler integration in two dimensions which is

$$\Delta t = 0.25c_p\rho(\Delta p)^2/\kappa. \quad (2.21)$$

### 3. The Stefan problem

The first example to be considered here is the Stefan problem in which a pure substance is cooled sufficiently for it to freeze. In the standard treatment of this problem the following condition is required at the interface

$$\kappa_1 \left( \frac{dT}{dy} \right)_1 - \kappa_2 \left( \frac{dT}{dy} \right)_2 = \rho L \frac{dY}{dt}, \quad (3.1)$$

where  $L$  is the latent heat/mass and  $dY/dt$  is the rate of change of the position of the interface [6]. The condition expresses the fact that the difference in the heat flux on each side of the interface supplies the heat to change the phase. In this formulation the position of the interface is one of the unknowns.

The SPH treatment of the freezing is very simple. Initially the SPH particles are placed on a grid which includes the boundary. They are assumed to be initially liquid and tagged with an integer to denote liquid particles and given the material properties of the liquid. As heat is conducted from the liquid some particles reach the solidification temperature  $T_m$ . The heat per unit mass  $q$  lost by these particles after this time is then stored and their temperatures are kept at  $T_m$ . If particle  $a$  is in this condition then, when  $q_a$  reaches  $L$ , the integer tag is changed to that for the solid phase, and the properties of this phase (thermal conductivity and heat capacity) are assigned to this particle. Between the solid particles and the liquid particles there is a region where the particles have reached the solidification temperature but have not yet had their latent heat fully extracted.

#### 3.1. The semi-infinite domain

The analytical solution [6] for a semi-infinite domain involves a parameter  $\lambda$  which is determined by the physical properties of the material and by the boundary conditions. If  $T_B$  is the fixed boundary temperature at  $y = 0$ , and  $T_0$  is the initial (uniform) temperature of the liquid, the analytical solution when the properties of the solid and liquid phases are equal gives the solid phase temperature profile

$$T(y) = T_B + \frac{(T_m - T_B)}{\text{erf}(\lambda)} \text{erf}(\eta), \quad (3.2)$$

and the liquid phase temperature profile

$$T(y) = T_0 + \frac{(T_m - T_0)}{\text{erfc}(\lambda)} \text{erfc}(\eta), \quad (3.3)$$

where  $\text{erf}(x)$  denotes the error function,  $\text{erfc}(x) = 1 - \text{erf}(x)$  and  $\eta$  is given by

$$\eta = y\sqrt{\rho C_p/(4\kappa t)}. \quad (3.4)$$

The interface is at

$$y = 2\lambda\sqrt{\kappa t/(\rho C_p)}, \tag{3.5}$$

and the parameter  $\lambda$  is given by

$$T_m - T_B = \text{erf}(\lambda)e^{\lambda^2} \left( \frac{\lambda L\sqrt{\pi}}{C} + \frac{(T_0 - T_m)e^{-\lambda^2}}{\text{erfc}(\lambda)} \right). \tag{3.6}$$

For test calculations it is convenient to specify  $\lambda$ ,  $T_m$  and  $T_0$  then use (3.6) to calculate  $T_B$ .

The system was assumed to be liquid in a unit square periodic in the  $x$  direction and with fixed temperatures at  $y = 0$  and  $y = 1$ . Although the  $y$  domain is finite the solution is close to the semi-infinite solution for the time we integrate the heat equation. The physical parameters were normalised so that  $c_p = 1$ ,  $L = 1$  and  $\kappa = 1$  for both the solid and liquid phases. The initial temperature was  $T_0 = 1.2$ , the melting temperature  $T_m = 1.0$ , and  $\lambda = 0.5$ . With these parameters  $T_B = 0.1906$ . The SPH equations with 40 particle spacings in each direction were integrated for 400 time steps when the time is 0.0568. The variation of temperature with  $y$  is shown in Fig. 1. The continuous curve shows the exact solution and the solid diamonds the SPH results. A sharp change in slope occurs at the interface between the ice and the liquid particles at  $y \sim 0.23$ .

There is good agreement between the exact and the SPH results. At any time some particles have reached the solidification temperature and then lost sufficient heat to become ice, and some have lost a negligible amount of heat and remain as liquid. The heat lost relative to the latent heat is shown in Fig. 2 where the particles which have not yet reached the melting temperature have been given the value zero. One line of particles has reached the solidification temperature but has only lost a fraction  $\sim 0.6$  of the latent heat. This figure shows that the interface occurs at  $y \sim 0.23$  which can be compared with the exact position  $y = 0.238$ . In Fig. 3 we shown the positions of the ice SPH particles and the liquid SPH particles.

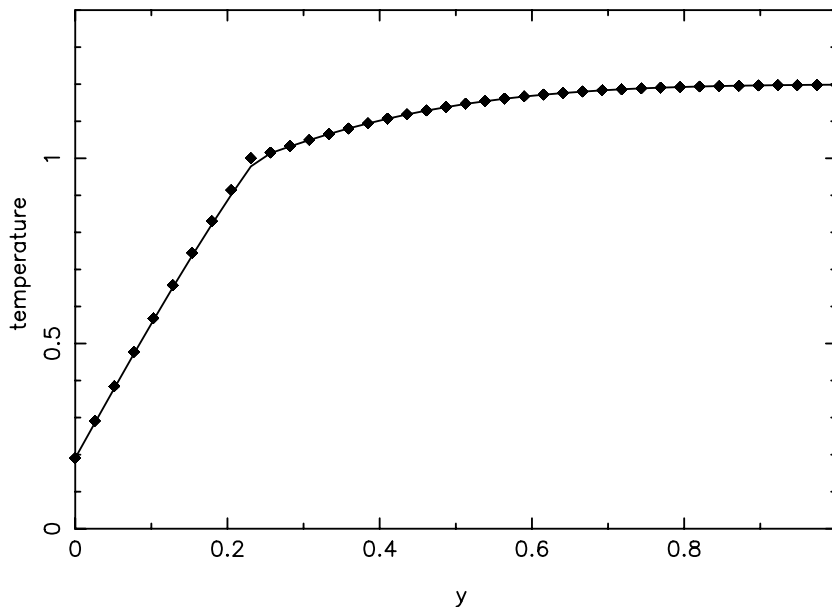


Fig. 1. The temperature against distance from the cooling boundary for a two dimensional Stefan problem. The system is periodic in the  $x$ -direction. The exact results are shown by the solid line and the SPH results by the solid diamonds. The change of slope shows the interface between solid and liquid.

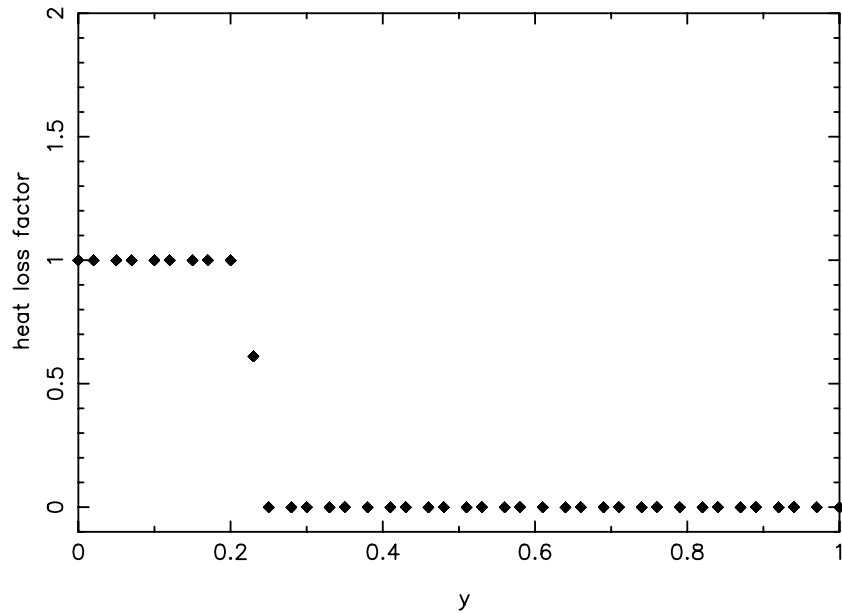


Fig. 2. The heat loss of particles relative to the latent heat  $L$  after reaching the melting temperature. The particles (liquid) which have not yet reached the melting temperature are assigned a zero value. The particles which have been cooled enough to change to ice have the value 1.0. One line of particles (a single point in this diagram) is at  $T_m$  but has not yet lost all its latent heat.

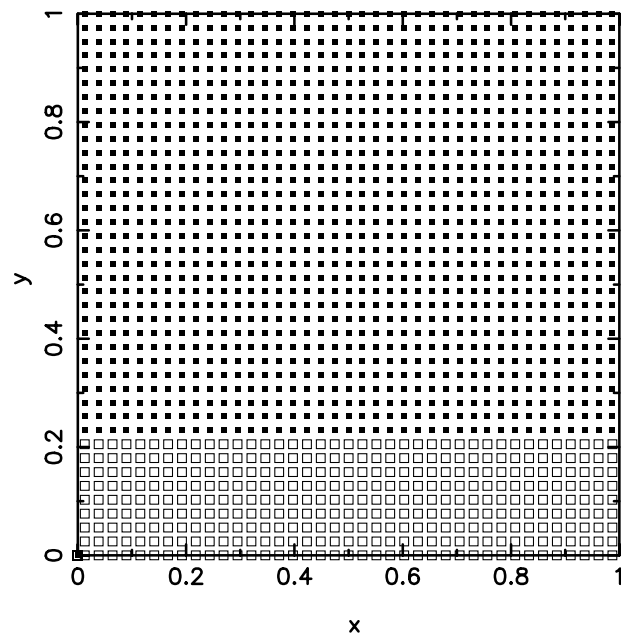


Fig. 3. The positions of the ice SPH particles (shown by open squares) and liquid SPH particles (shown by filled squares).

### 3.2. Conduction with heat sinks

We now consider the case of a liquid in two dimensions cooled by a point heat sink of strength  $Q$  (to conform with the theoretical solution we use a positive  $Q$  in the equations below, but in the SPH equations it is negative). The theoretical solution for this case is given by Carslaw and Jaeger [6]. If  $R = 2\lambda\sqrt{\hat{\kappa}_s t}$  denotes the radial coordinate of the interface between the solid (ice) and the liquid at any time  $t$ . The melting (or freezing temperature) is denoted by  $T_{\text{melt}}$  and  $T_\infty$  denotes the temperature far from the heat sink. The temperature of the solid in  $r < R$  is given by

$$T_s = T_{\text{melt}} + \frac{Q}{4\pi\hat{\kappa}_s} \left[ E_1(\lambda^2) - E_1\left(\frac{r^2}{4\pi\hat{\kappa}_s t}\right) \right], \tag{3.7}$$

where  $\hat{\kappa} = \kappa/(\rho c_p)$  and  $E_1(z)$  is the exponential integral defined by

$$E_1(z) = \int_z^\infty \frac{\exp -u}{u} du. \tag{3.8}$$

The temperature of the liquid in  $r > R$  is given by

$$T_\ell = T_\infty - \frac{(T_\infty - T_{\text{melt}})}{E_1(\lambda^2\hat{\kappa}_s/\kappa_\ell)} E_1\left(\frac{r^2}{4\pi\hat{\kappa}_s t}\right), \tag{3.9}$$

and  $\lambda$  is the root of the equation

$$\frac{Q}{4\pi} e^{-\lambda^2} - \frac{\kappa_\ell(T_\infty - T_{\text{melt}})}{E_1(\lambda^2\hat{\kappa}_s/\hat{\kappa}_\ell)} e^{-\lambda^2\hat{\kappa}_s/\hat{\kappa}_\ell} = \hat{\kappa}_s L \rho \lambda^2. \tag{3.10}$$

In practice, we specify  $T_\infty$ ,  $T_{\text{melt}}$  and  $\lambda$  and use the previous equation to fix  $Q$ .

We apply the SPH equation to simulate water placed in a square domain of side 1 m with a source at the centre of the square. We take the thermal conductivity and heat capacity of the water in SI units to be 0.591 and 4190, respectively. The corresponding values for ice were taken as 2.20 and 4190. The latent heat of fusion is  $3.335 \times 10^5$  J/kg and we take the density of both phases to be  $10^3$  kg/m<sup>3</sup>. We take  $T_\infty = 10$  and  $T_{\text{melt}} = 0$ . We write  $Q$  for the exact solutions in the form  $q' L \rho \hat{\kappa}_s$  and calculate  $q'$  from (3.10).

In the first simulation we take  $\lambda = 0.15$  and find  $q' = 0.03365$  because we have a sink the value of  $Q$  in (2.9) is negative with magnitude  $q' L \rho \hat{\kappa}$ . We place the SPH particles on a square grid using a total of 1600 particles and take  $h = 1.3\Delta p$  where  $\Delta p$  is the particle spacing. The particles are shown in Fig. 4 after 3000 time steps (equal to a time elapse of 132 h). The ice particles are shown by open circles. The boundary of the ice is irregular but, as is clear from the figures, the variation of the physical properties is very close to radial. For example, Fig. 6 shows the temperature of all particles. If there was a non radial variation it would show up in a spread of the SPH results around the theoretical curve.

Fig. 5 shows the heat loss factor defined as the heat loss after the temperature of the liquid particle first reaches  $T_{\text{melt}}$ . It is scaled to  $L$  and is set to 1 after the SPH particle changes from water to ice. The exact value of  $R$  is 0.212, which is in satisfactory agreement with the position of the interface in the simulation given by approximately 0.22. This figure shows that, in front of the ice, there is a thin region consisting of those liquid particles which have reached the melting temperature, but which have not yet lost their latent heat. Fig. 6 shows the temperature profile. The agreement is very satisfactory with the largest errors occurring in the ice. Just beyond the interface between the ice and the liquid at a radius  $\sim 0.22$  there is a thin layer (approximately 2 particle spacings thick) of liquid particles which have reached the melting temperature but have not yet lost their latent heat. The presence of such a narrow interface region is also found in enthalpy methods [8].

Fig. 7 shows the temperature in a simulation with 2500 ( $50 \times 50$ ) particles. The improvement in accuracy compared with Fig. 6 in the ice region  $0 < r < 0.21$  is clear.

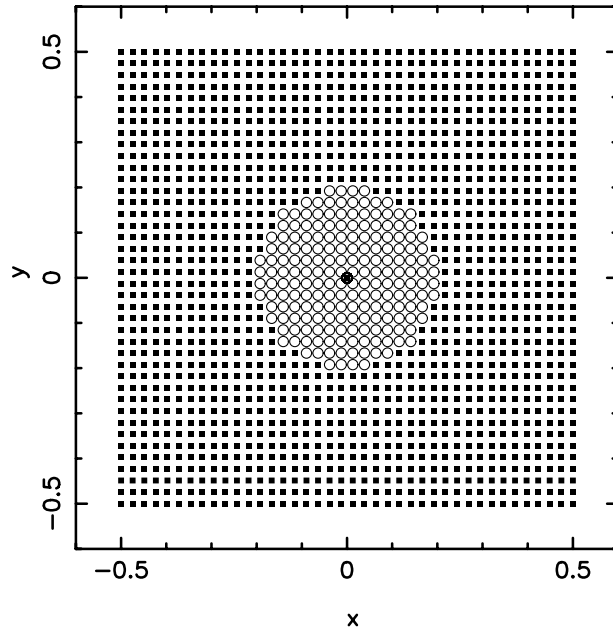


Fig. 4. The coordinates of SPH particles for the case  $\lambda = 0.15$  with a delta function heat sink at the origin. The ice particles are shown as open circles and the liquid particles and solid squares. Although the interface between the ice and the liquid looks irregular the variation of the properties is very close to radial.

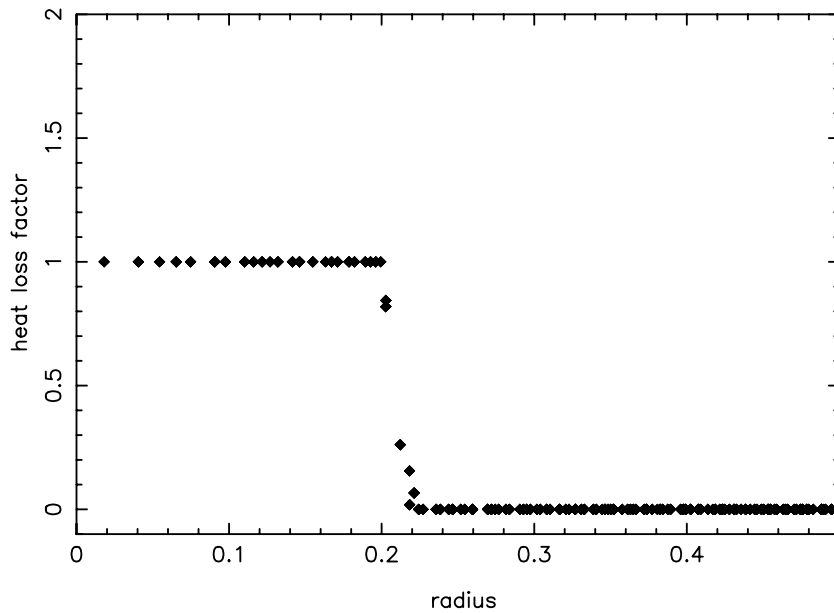


Fig. 5. The heat loss factor against radius for the case of a heat sink at the origin. Note the thin layer of liquid particles which have not yet lost all their latent heat but have in fact reached  $T_{\text{melt}}$ . The exact interface distance is at  $R = 0.212$ .

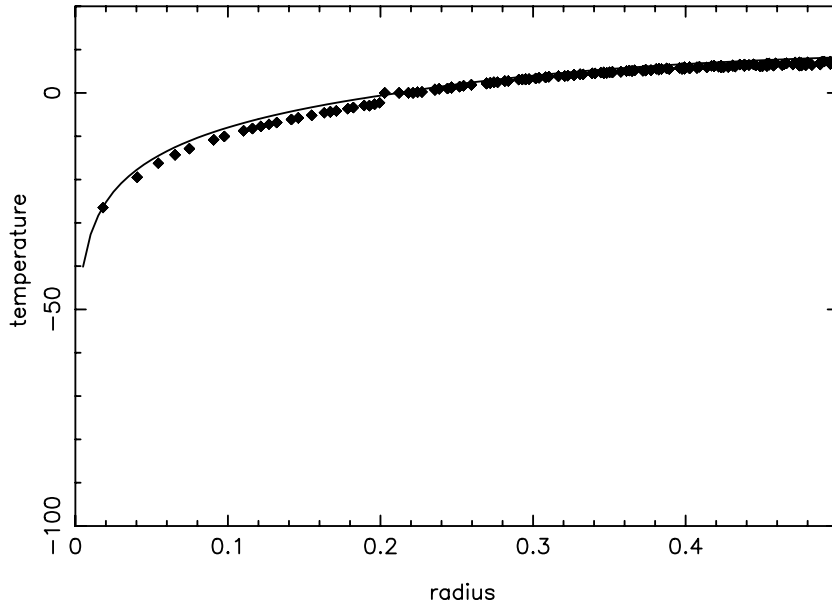


Fig. 6. The temperature against radius for the case  $\lambda = 0.15$  with 1600 particles ( $40 \times 40$ ). The exact results are shown by the continuous line and the SPH results by symbols. Despite the particles being on a rectangular grid the variation of the temperature is close to radial. Note the small group of particles which have reached the freezing temperature but have not yet become ice particles. These form a small horizontal line at a radius of approximately 0.22.

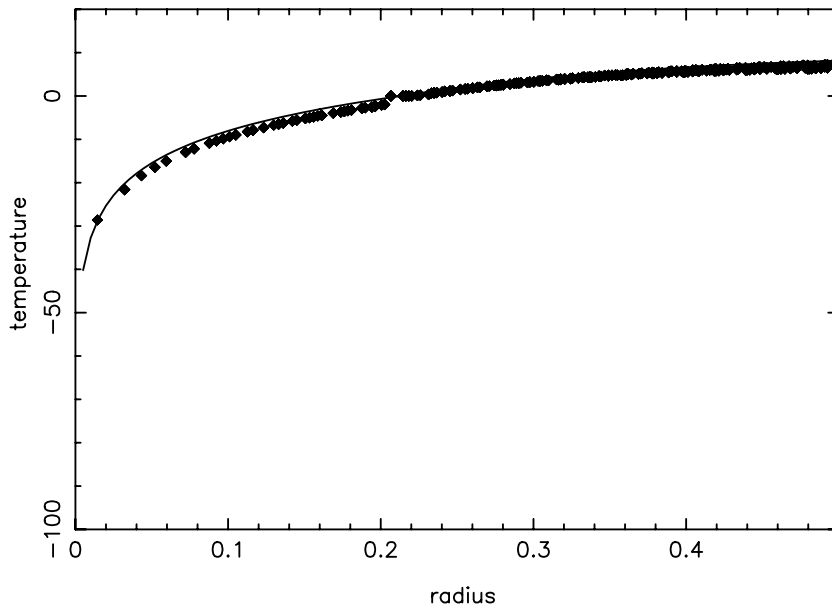


Fig. 7. The temperature against radius for the case  $\lambda = 0.15$  but with 2500 particles ( $50 \times 50$ ). The exact results are shown by a continuous line and the SPH results by symbols. Compared to Fig. 6 there is a clear improvement in accuracy in the ice region  $0 < r < 0.21$ .

Table 1  
Table showing the mean square error in the interface radius for various  $nx$

Error-1	Error-2	$N$
0.01063	0.0167	20
0.00544	0.00840	30
0.00370	0.00548	40
0.00275	0.00407	50

Error-1 is based on the maximum radius of the ice particles +0.5 h, and Error-2 denotes the maximum radius of particles with heat loss factor  $>0.25L$ .

The improvement in accuracy with increased particle number can also be seen from Table 1 where the values of the mean square deviation of the interfacial radius are given for various  $N$  where  $N$  denotes the number of particles along the side of the square domain. This error is based on at least 50 interface estimates for each resolution. The error in the radius is due to intrinsic numerical errors, for example the fact that initial delta function source has been smoothed over  $2h$ . In addition the interface is only defined approximately because liquid particles close to the interface have nearly, but not entirely, lost their latent heat. The interface radius was therefore calculated in two ways. First by adding  $0.5h$  to the maximum radius of ice particles (denoted Error-1) and by taking the maximum radius for particles with heat loss factor  $>0.25$  (denoted by Error-2). This latter radius is roughly between the fully ice and fully liquid particles.

The resulting error varies with  $h$  approximately as  $h^{1.7}$ . In Fig. 8, we show the radius against time for three resolutions. The improvement in accuracy with resolution is clear.

Qualitatively similar results occur for a stronger sink. We take  $\lambda = 0.20$  and find  $q' = 0.055928$ . We use 1600 particles and integrate for 2000 steps (equivalent to a time lapse of 88 h). At this time the exact  $R = 0.2309$  which is in satisfactory agreement with the mid point of the smoothed interface shown in

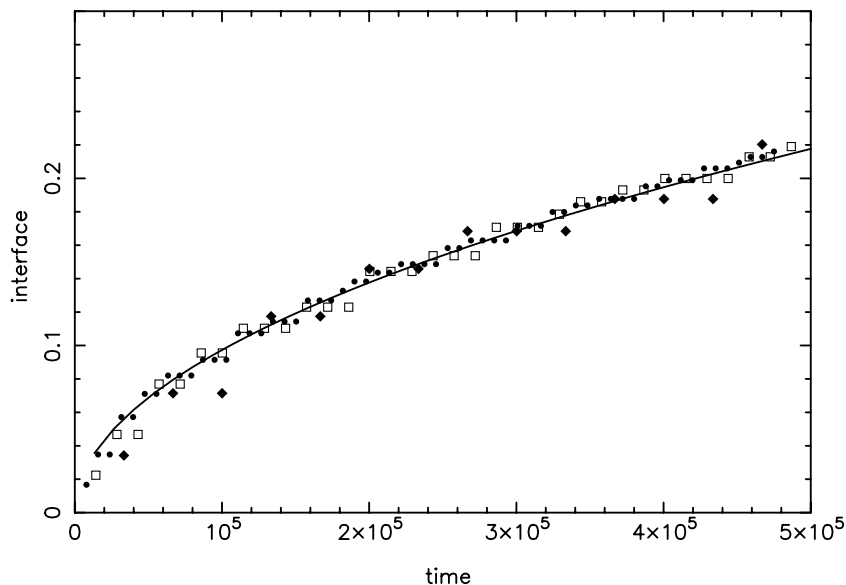
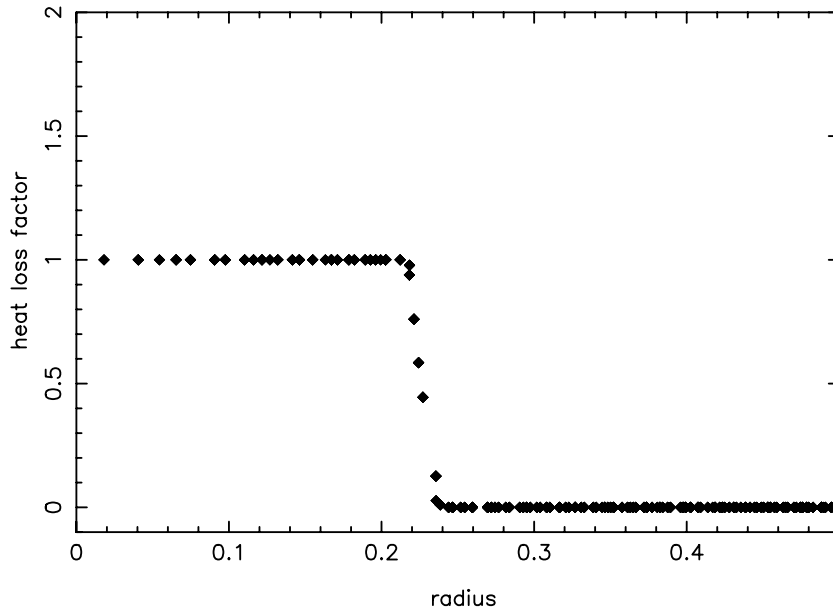
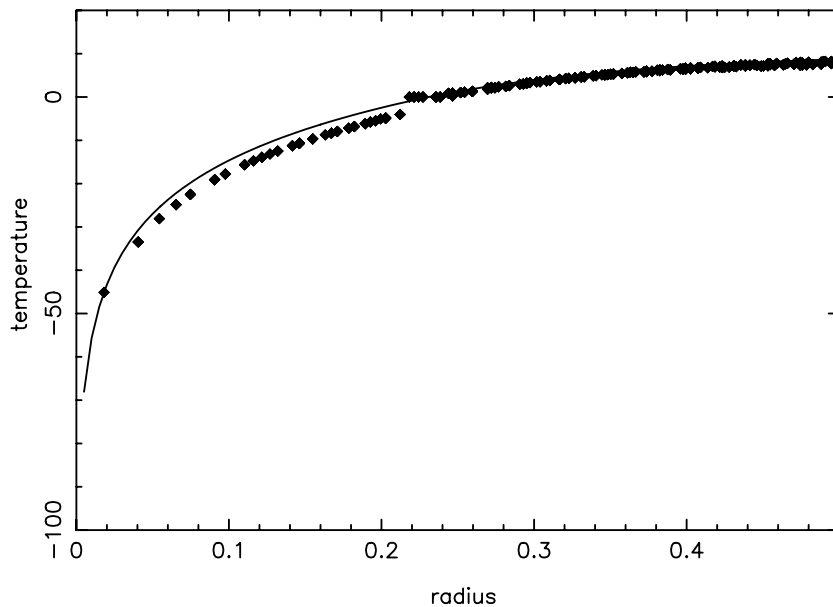


Fig. 8. The interface radius against time (in seconds) for the case  $\lambda = 0.15$  with 400 particles (filled diamonds), 900 particles (open squares) and 1600 particles (filled circles). The exact result is shown by the continuous line.

**Fig. 9.** In Fig. 10, we show the temperature profile at the same time as for Fig. 9. As with the weaker sink, the accuracy is better in the liquid region and is comparable to that with the weaker sink for the same number of particles.



**Fig. 9.** The heat loss factor against radius for the case  $\lambda = 0.20$  with 1600 particles ( $40 \times 40$ ).



**Fig. 10.** The temperature against radius for the case  $\lambda = 0.20$  with 1600 particles ( $40 \times 40$ ). The exact results are shown by a continuous line and the SPH results by symbols.

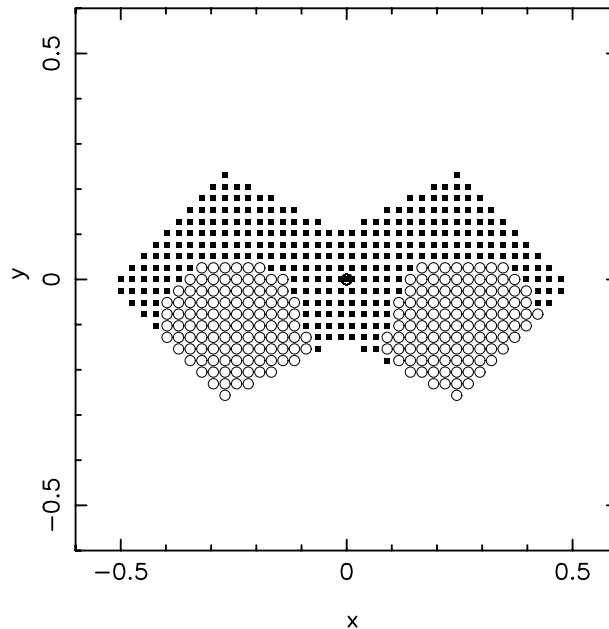


Fig. 11. The coordinates of SPH particles for the case of two heat sinks with coordinates  $x = \pm 0.25$  and  $y = -0.1$  in an irregular enclosure. The ice particles are denoted by open circles and the liquid particles by filled squares.

We now consider the freezing of water in an irregular, adiabatic enclosure roughly modelling a cavity with nearly bilateral symmetry. We take the strengths of the sinks to be equal and the parameter  $q' = 0.03665$ . With many numerical methods the imposition of an irregular enclosure requires careful, time consuming, differencing near the boundary. The advantage of SPH is that we can use the same program as before but with a different particle placement. In this case we place two heat sinks with  $q = 0.033651$  at  $x = \pm 0.25$  and  $y = -0.1$ . The particle placement is approximately symmetric about the  $y$ -axis.

The positions of the particles at an early stage of the freezing are shown in Fig. 11. At this time the liquid has frozen around the sinks down to the bottom boundary. At a later time (not shown) the liquid is confined to a small region near the upper boundary.

These results show that our SPH formulation of solidification is easy to use and gives very satisfactory results for both configurations in rectangular boundaries, where analytical results are available, and for irregular boundaries where the immediate issue is the ease with which boundaries can be incorporated to give results that are physically reasonable.

#### 4. The freezing of a salt solution

We now consider the more complicated problem of the freezing of an aqueous salt solution. In this case, when an element of the liquid solution reaches the liquidus temperature  $T_L$ , further loss of heat results in some ice being formed and the concentration of salt in the solution increases. This problem was considered by Wollhöver et al. [27] assuming the interface between ice and solution was sharp. However, the conditions they assumed rapidly produce an unstable interface which then produces a mush comprising a mixture of dendritic ice crystals and solution (see for example [15]). The same problem was used as a test case by Udaykumar and Mao [24] again assuming the interface was sharp. The SPH method, as mentioned earlier, does

not assume the interface is sharp, but instead approximates the formation of the mush between the ice and the solution. In this respect, like most enthalpy methods, our technique does not allow disequilibrium (constititional supercooling) in the system.

At any time the freezing solution will be a mixture of ice SPH particles with different masses, and liquid (solution) SPH particles with different masses. As a consequence, the density of the liquid or solid will not be the intrinsic density  $\rho$  of the phase but a lower density  $\hat{\rho}$  related by the volume fraction  $\theta$  according to  $\hat{\rho} = \theta\rho$ . Correspondingly, the thermal conductivity for each phase is replaced by  $\hat{\kappa} = \theta\kappa$ . The heat conduction equation for any particle, ice or liquid, then takes the form

$$\mathcal{C}_p \frac{dT}{dt} = \frac{1}{\hat{\rho}} \nabla(\hat{\kappa} \nabla T), \tag{4.1}$$

with the SPH equation

$$c_{p,a} \frac{dT_a}{dt} = \sum_b \frac{m_b}{\hat{\rho}_a \hat{\rho}_b} \frac{4\hat{\kappa}_a \hat{\kappa}_b}{(\hat{\kappa}_a + \hat{\kappa}_b)} (T_a - T_b) F_{ab}. \tag{4.2}$$

From (4.2) we can easily show that the SPH equation conserves the total heat of an isolated set of particles because

$$\sum_a m_a c_{p,a} \frac{dT_a}{dt} = \sum_a \sum_b \frac{m_a m_b}{\hat{\rho}_a \hat{\rho}_b} \frac{4\hat{\kappa}_a \hat{\kappa}_b}{(\hat{\kappa}_a + \hat{\kappa}_b)} (T_a - T_b) F_{ab} \tag{4.3}$$

is zero. If  $a$  denotes an ice or liquid SPH particle then it can exchange heat with all other neighbouring particles ice or liquid. The summation in (4.2) therefore is over all neighbouring particles  $b$  with their appropriate  $\hat{\kappa}_b$  and  $\hat{\rho}_b$ .

The salt diffusion equation has the same form as before except that  $\rho$  is replaced by  $\hat{\rho}$  and the diffusion coefficient  $D$  is replaced by  $\theta D$ . It is straightforward to show that this equation conserves the total amount of salt. In the problems considered in this paper the diffusion equation only applies to the liquid SPH particles since the ice is assumed to be salt free. This assumption is not essential. The argument leading to the increase of entropy from heat conduction and compositional change still applies.

This formulation has some of the features of the mushy layer formulation. However, instead of treating the mushy layer as a continuum with properties which depend on the volume fraction, we treat the solid SPH particles as one fluid, and the liquid SPH particles as another fluid, but allow for the fact that they can be interspersed within each other.

#### 4.1. Thermodynamics

Consider a liquid SPH particle of mass  $m$  with salt concentration  $C$ . Suppose it was at the liquidus temperature and in the next time step it loses an amount of heat  $q$  per unit mass. A mass  $m_{ice}$  of ice will be formed and the temperature will decrease by  $|\Delta T|$ . Since the thermal energy must be conserved the heat lost  $qm$  must equal the heat extracted to form the ice plus the heat associated with the thermal change of the remaining salty liquid. This takes the form

$$qm = m_{ice}L + m_{ice}C_p^{ice}|\Delta T| + (m - m_{ice})C_p^{liq}|\Delta T|. \tag{4.4}$$

The liquidus equation allows us to relate the change in concentration (and therefore  $m_{ice}$ ) to the change in temperature. The mass of salt is  $Cm$  (we assume this stays in the liquid) so that the salt concentration in the liquid particle becomes

$$C + \Delta C = \frac{Cm}{m - m_{ice}}, \tag{4.5}$$

and then

$$\Delta C = \frac{C m_{\text{ice}}}{m - m_{\text{ice}}}. \quad (4.6)$$

From the liquidus equation (which we assume to be linear for simplicity but arbitrary forms can easily be included) we have

$$\Delta T = -\Gamma \Delta C, \quad (4.7)$$

and combining (4.6) and (4.7) we get

$$m_{\text{ice}} = \frac{|\Delta T|(m - m_{\text{ice}})}{\Gamma C}, \quad (4.8)$$

or

$$m_{\text{ice}} = \frac{m|\Delta T|}{\Gamma C + |\Delta T|}. \quad (4.9)$$

We could solve for  $|\Delta T|$  by substituting the previous expression for  $m_{\text{ice}}$  into (4.4) which gives a quadratic equation for  $|\Delta T|$ . However, in more complicated problems this is not possible. We therefore chose to solve for  $|\Delta T|$  using the following iterative method.

Making use of the previous equation we can write (4.4) in the form

$$|\Delta T| = q / \left( L + (C_p^{\text{ice}} - C_p^{\text{liq}}) |\Delta T| \left( 1 - \frac{m_{\text{ice}}}{m} \right) / (\Gamma C) + C_p^{\text{liq}} \right). \quad (4.10)$$

This equation (together with (4.9)) can be solved by iteration using the initial values  $|\Delta T| = 0$  and  $m_{\text{ice}} = 0$ . The iterations were stopped when the absolute value of the change in  $m_{\text{ice}}$  between two iterations, relative to the average value of  $m_{\text{ice}}$  for the two iterations, was  $< 0.001$ .

#### 4.2. Mapping the new ice to the ice particles

After the amount of new ice formed has been determined it must be mapped to neighbouring ice SPH particles. In the following the subscripts  $a$  and  $b$  will be reserved for the liquid particles and  $i$  and  $j$  for the ice particles.

First we note that  $\hat{\rho}_a$  is given by

$$\hat{\rho}_a = \sum_b m_b W_{ab}, \quad (4.11)$$

and in the present problem  $\hat{\rho}$  only changes because the mass of the liquid particles can change.

The change in mass of the ice particle  $j$  is due to the ice formed from neighbouring liquid particles cooled along the liquidus. If the ice formed by particle  $a$  is denoted by  $\Delta m_a$  then the change in mass of ice particle  $j$  can be obtained from the approximate interpolation formula

$$\Delta m_j = \sum_a \Delta m_a \zeta_a W_{aj}, \quad (4.12)$$

where the factor  $\zeta_a$  normalises the interpolation formula so that the total new mass of ice is equal to the decrease in mass of the liquid. Thus, from (4.11)

$$\sum_j \Delta m_j = \sum_a \Delta m_a \zeta_a \sum_j W_{aj}. \quad (4.13)$$

We therefore choose

$$\zeta_a = \frac{1}{\sum_j W_{aj}}, \tag{4.14}$$

so that mass will be conserved. In our calculations the mass is conserved to within round off error.

In addition to conserving mass we need to consider the effect of the mapping on the temperature. The ice SPH particle receives ice from liquid particles which may be at slightly different temperatures. The heat in ice particle  $j$  is

$$(m_j + \Delta m_j)C_{p,j}T'_j = m_jC_{p,j}T_j + \sum_a \Delta m_a C_{p,a}T_a \zeta_a W_{aj}, \tag{4.15}$$

where  $T'_j$  is the temperature of ice particle  $j$  after the mass is transferred. In this expression, we use the same normalizing factor  $\zeta$  we used for the mass normalization. With this factor included, the total thermal energy after this transfer

$$\sum_j (m_j + \Delta m_j)C_{p,j}T'_j \tag{4.16}$$

is equal to the thermal energy before the transfer plus the transferred thermal energy

$$\sum_j m_j C_{p,j} T_j + \sum_a \Delta m_a C_{p,a} T_a. \tag{4.17}$$

### 4.3. Density and volume fraction

The average density  $\hat{\rho}_j$  of ice particle  $j$  is given by

$$\hat{\rho}_j = \sum_k m_k W_{jk}, \tag{4.18}$$

where the summation is over the neighbouring ice particles.

The rate of change of this density, in the general case where the particles can move, is

$$\frac{d\hat{\rho}_j}{dt} = \sum_k m_k (\mathbf{v}_j - \mathbf{v}_k) \cdot \nabla W_{jk} + \sum_k \frac{dm_k}{dt} W_{jk}. \tag{4.19}$$

The first term on the right hand side is the SPH expression of

$$-\hat{\rho} \nabla \cdot \mathbf{v}, \tag{4.20}$$

evaluated at the position of particle  $j$ . Together with the term on the left hand side it gives the usual continuity equation when the particles have fixed mass. The second term on the right hand side is the change in density associated with the change in the masses of the particles. For the problems considered here the velocity is zero and only the change in  $\hat{\rho}$  due to the mass change is required. A similar equation applies to the liquid particles. The change in the initial values computed to first order using (4.18) is

$$\Delta \hat{\rho}_j = \sum_k \Delta m_k W_{jk}. \tag{4.21}$$

The new volume fraction  $\theta_j$  of ice particle  $j$  is then given by

$$\theta_j = \frac{\hat{\rho} + \Delta \hat{\rho}_j}{\rho_{\text{ice}}}, \tag{4.22}$$

where  $\rho_{\text{ice}}$  is the fixed density of ice. The intrinsic density  $\rho_a$  of liquid particle  $a$  in general changes during the evolution of the system because the concentration of salt in the solution increases when ice is formed. While

we could take this into account we prefer to calculate the volume fraction of the liquid in the following way. At the position of a liquid particle we can estimate the average density of the ice and thus determine  $\theta$  of the ice at the position of an SPH liquid particle. This is, in fact, an estimate of the ice  $\theta$  in the neighbourhood of the liquid particle. We denote it by  $\theta_a(\text{ice})$ . The volume fraction of the liquid at the position of  $a$  is then

$$\theta_a = 1 - \theta_a(\text{ice}), \quad (4.23)$$

where, following the previous remarks

$$\theta_a(\text{ice}) = \frac{\sum_k m_k W_{ka}}{\rho_{\text{ice}}}, \quad (4.24)$$

and the summation is over ice particles.

## 5. Application to a freezing sodium nitrate solution

The equations described above were tested by applying them to the freezing of a solution of sodium nitrate in water [12]. The particular case we consider is with initial salt concentration 0.14, bottom cold boundary at  $-16.5^\circ\text{C}$ , and the fluid at  $14.7^\circ\text{C}$ . The sides are assumed to be perfectly insulated. We use SI units for which  $L = 334.4 \times 10^3 \text{ J/kg}$ , the heat capacity of water is  $4180 \text{ J/(kg K)}$ , and the heat capacity of ice is  $2006 \text{ J/(kg K)}$ . The thermal conductivity of ice is 2.408 and that of water is 0.498 with units  $\text{J/(ms)}$ . The diffusion coefficient of the salt is  $6.8 \times 10^{-7} \text{ kg/(ms)}$ . The initial density of the solution is estimated from the contours in Fig. 1 of the paper by Huppert and Worster [12]. The value of the parameter  $\Gamma$  for the liquidus was estimated from the CRC tables as  $42.28 \text{ (K/kg)}$ . The solution is assumed to be in a square container of side 0.5 m.

The SPH particle configuration was set up on a grid with virtual ice particles in the same position as the liquid particles except at the cold boundary. Because it is convenient to use particles to fix the boundary it is necessary to decide what sort of particles will be on the cold boundary. If we choose them to be liquid particles then we cannot consistently keep them at the cold boundary temperature because at this temperature they should be ice particles. We therefore assume that a layer of ice quickly forms on the cold boundary and we represent this by a line of ice particles with a temperature which is fixed at the boundary temperature. In the calculations presented here  $h = 1.3\Delta p$  and the number of particles used was  $30 \times 30$ .

In Fig. 12, the temperature is shown as a function of distance measured from the cold boundary. The lower curve is after 3 h and 40 min and the upper curve is at 25 h and 35 min. The SPH results are shown by  $X$ , the experimental values are shown by diamonds, and the results from mushy layer theory [4] are shown by the continuous curve. The agreement between the SPH, the mushy layer theory, and the experimental results at the time 3 h and 40 min is very good. The results from both SPH and the mushy layer theory for the time 25 h and 35 min are, however, shifted from the experimental so that, at any height, the SPH temperature is lower than in the experiment. A possible explanation of the errors over  $\sim 24 \text{ h}$  is a transfer of heat from the laboratory with a temperature of  $20^\circ\text{C}$  to the nitrate solution with a typical average temperature of around  $0^\circ\text{C}$ .

Fig. 13 shows the volume fraction for the ice (shown as a diamond), the liquid particles (shown by open circles), and the mushy layer theory (shown by a continuous curve) after 25.5 h. The mushy layer theory agrees satisfactorily with the SPH solution for high ice volume fractions but decreases more rapidly to zero than the SPH results. The difference may be due to the fact that there are differences in the temperature between the two calculations at this time. However, it may also be partly due to the smoothing inherent in the SPH calculations. To illustrate this we smoothed the mushy layer volume fraction using the same kernels as for the SPH calculations. The results are shown by the solid stars. It is clear that the smoothed mushy layer results vary in a way which is similar to the SPH though the magnitude is different as is to be

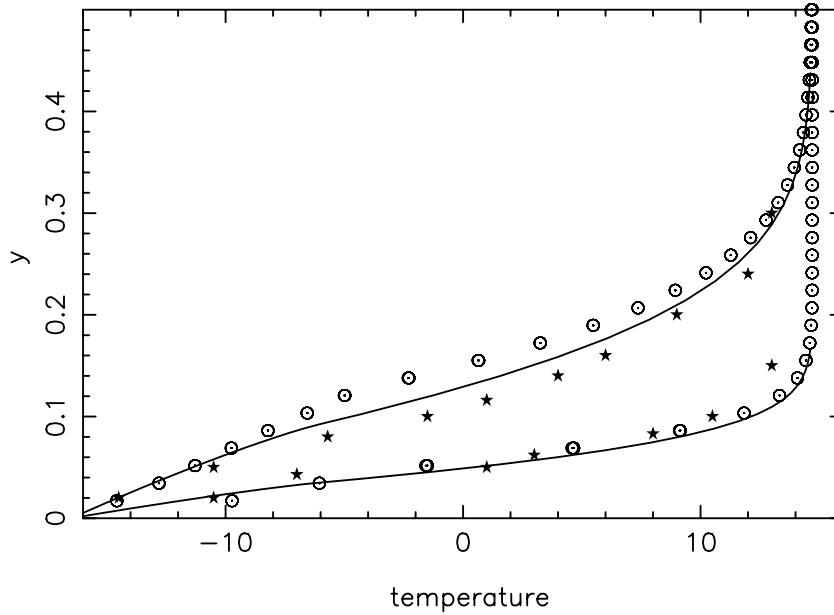


Fig. 12. Temperature against distance from the cooling boundary. The experimental results are shown by filled circles, the SPH results by open circles, and the mushy layer theory by the continuous curve. The lower curves and data points are after 3 h and 40 min. The upper curves and data points are after 25 h and 30 min.

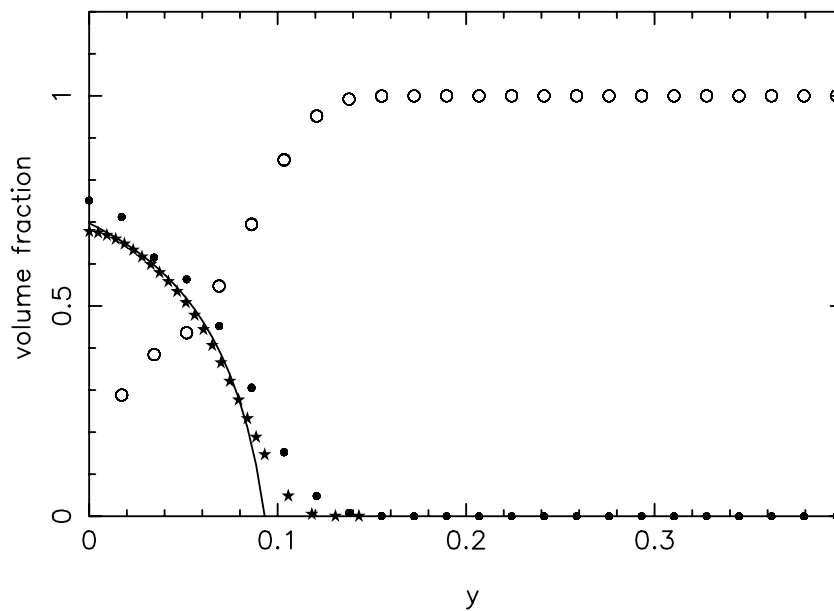


Fig. 13. The volume fraction of ice and liquid as a function of distance  $y$  from the cooling boundary at the time 25.5 h. Values for ice shown by solid circles, values for the solution are shown by  $O$  and the result of the mushy layer theory is shown by a continuous curve. The solid stars denote the smoothed mushy layer curve.

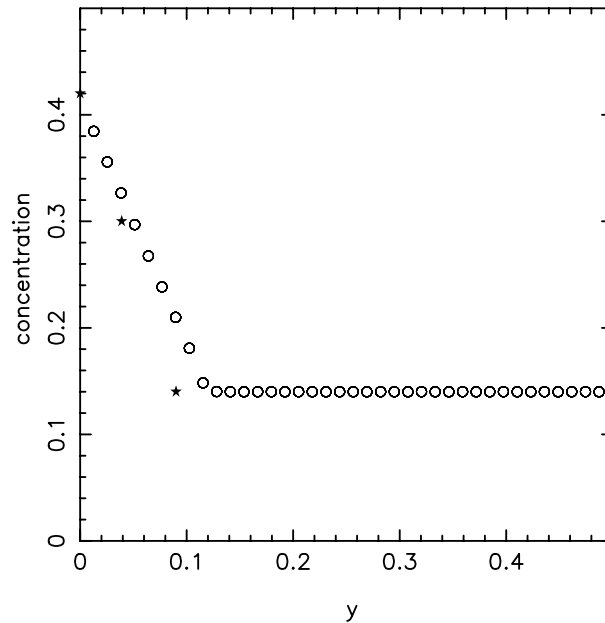


Fig. 14. The salt concentration as a function of distance  $y$  from the cooling boundary. The mushy layer results are shown by solid stars. The SPH results are shown by open circles.

expected from the temperature differences between the two calculations at this time. Finally, in Fig. 14, we show the salt concentration at the same times as a function of depth. The results are very close to the mushy layer results which are shown by 3 points (solid stars).

These results show that the SPH formulation of the freezing problem for a binary solution is satisfactory and is in good agreement with the mushy layer results.

## 6. Discussion and conclusions

In this paper, we have shown that it is possible to devise an extension of the SPH method which gives a robust algorithm for solidification problems. The SPH equations for both heat conduction and salt diffusion can be solved without reference to the interface between the solid and liquid phases. The method is simple to use and guarantees both energy conservation and the increase of entropy from both thermal conduction and from salt diffusion in the absence of sources. The method can be trivially extended to handle the solidification of ternary and higher order alloy systems, which are common in both industrial and natural contexts, but where investigation has only just begun [1,20].

The results for solidification of a homogeneous liquid are very satisfactory both for freezing in a regular domain, where analytical results are available, and in irregular domains. In the latter case no changes to the code are required to deal with boundary conditions on the irregular boundary.

A comparison of the temperature from experiment and mushy layer theory for an aqueous nitrate solution at sub-eutectic concentration gives good agreement for times  $\sim 4$  h. For later times  $\sim 24$  h the agreement is less satisfactory. We suggest, in the latter case, that slow conduction of heat from the laboratory to the experimental apparatus is the explanation of the differences between SPH and experimental results. Our results for the volume fraction of the ice and liquid have been compared against the mushy layer

theory. We find reasonable agreement, which is improved if the mushy layer results are smoothed so as to be consistent with the SPH results.

The experimental results for the salt concentration have significant errors for samples drawn from deep within the solution. As a result neither the SPH results nor the results from mushy layer theory agree with experiment for the layers close to the ice-liquid interface. The agreement elsewhere is good.

There are numerous extensions to the present algorithm which we are now considering. These include the important problem of simulating bulk motion driven by the density differences due to the salt in the liquid, and the density difference between the solid and liquid phases.

## Acknowledgments

We thank the EPSRC for a grant which supported JJM to work in Cambridge on this problem. This paper was partially completed while one of the authors (HEH) was a Gledden Fellow at the University of Western Australia. He is grateful to Jorg Imberger and the members of the Centre for Water Resources for the kindness and stimulation he enjoyed.

## References

- [1] A. Aitta, H.E. Huppert, M.G. Worster, *J. Fluid Mech.* 440 (2001) 359–380.
- [2] D.R. Athey, *J. Inst. Math. Appl.* 13 (1974) 353.
- [3] C. Beckerman, H.-J. Hiepers, I. Steinback, A. Karma, X. Tong, *J. Computat. Phys.* 154 (1999) 468.
- [4] A.O.P. Chiareli, H.E. Huppert, M.G. Worster, *J. Crystal Growth* 139 (1994) 134–146.
- [5] A.B. Crowley, J.R. Ockendon, *J. Inst. Math. Appl.* 20 (1977) 269.
- [6] H.S. Carslaw, J.C. Jaeger, *Conduction of Heat in Solids*, Publisher Oxford Press, Oxford, 1990.
- [7] P.W. Cleary, J.J. Monaghan, *J. Computat. Phys.* 148 (1999) 227.
- [8] J. Crank, *Free and Moving Boundary Problems*, Oxford Science Publications, Oxford, UK, 1987.
- [9] M.E. Glicksman, *Ann. Rev. Fluid. Mech.* 18 (1986) 307.
- [10] H.E. Huppert, *J. Fluid Mech.* 173 (1986) 557–594.
- [11] H.E. Huppert, *J. Fluid Mech.* 212 (1990) 209–240.
- [12] H.E. Huppert, G. Worster, *Nature* 314 (1985) 703.
- [13] D. Juric, in: B.G. Thomas, C. Beckermann (Eds.), *Modeling of Casting, Welding and Solidification Processes*, eighth ed., TMS, 1998, pp. 605–612.
- [14] Juric, D., Tryggvason, G., 1996. Heat transfer in Microgravity Systems, HTD-332, ASME 33–44.
- [15] Ch. Körber, W. Scheiwe, K. Wollhöver, *Int. J. Heat Mass Transfer* 26 (1983) 1241–1253.
- [16] J.J. Monaghan, *Ann. Rev. Astron. Astrophys.* 30 (1992) 543.
- [17] O.A. Oleinik, *Sov. Math. Dokl.* 1 (1960) 1380.
- [18] A.N. Parshikov, S.A. Medin, *J. Computat. Phys.* 180 (2002) 358.
- [19] C. Peskin, *J. Computat. Phys.* 25 (1977) 220–252.
- [20] A. Thompson, H.E. Huppert, M.G. Worster, A. Aitta, *J. Fluid Mech.* 497 (2003) 167–199.
- [21] R. Tonhardt, G. Amberg, *J. Crystal Growth* 194 (1998) 406.
- [22] G. Tryggvason, B. Bunner., A. Esmaeeli, D. Juric, N. Al-Rawahi, W. Tauber, S. Han, S. Nas, Y.-J. Jan, *J. Computat. Phys.* 169 (2001) 708.
- [23] Tsiveriotis, R.A. Brown, *Int. J. Numer. Meth. Fluids* 14 (1992) 981–1003.
- [24] H.S. Udaykumar, L. Mao, *Int. J. Heat Mass Transfer* 45 (2002) 4793–4808.
- [25] L.H. Ungar, R.A. Brown, *Phys. Rev. E* 31 (1985) 1931.
- [26] L.H. Ungar, R.A. Brown, *Phys. Rev. B* 29 (1984) 1367–1380.
- [27] K. Wollhöver, Ch. Körber, M.W. Scheiwe, U. Hartmann, *Int. J. Heat Mass Transfer* 28 (1985) 761–769.
- [28] M.G. Worster, *J. Fluid Mech.* 167 (1986) 481–501.
- [29] M.G. Worster, *The dynamics of mush layers*, in: S.H. Davis (Ed.), *Interactive Dynamics of Convection and Solidification*, Publisher Kluwer, Netherlands, 1992, pp. 113–138.